Neurobiology of Aging 53 (2017) 48–58

Contents lists available at ScienceDirect

Neurobiology of Aging

journal homepage: www.elsevier.com/locate/neuaging

# Traffic-related air pollution impact on mouse brain accelerates myelin and neuritic aging changes with specificity for CA1 neurons

Nicholas C. Woodward [a], Payam Pakbin [b], Arian Saffari [b], Farimah Shirmohammadi [b], Amin Haghani [a], Constantinos Sioutas [b], Mafalda Cacciottolo [a], Todd E. Morgan [a], Caleb E. Finch [a,c,*]

[a] Leonard Davis School of Gerontology, University of Southern California, Los Angeles, CA, USA
[b] Department of Civil and Environmental Engineering, Viterbi School of Engineering, University of Southern California, Los Angeles, CA, USA
[c] Department of Molecular and Computational Biology, Dornsife College, University of Southern California, Los Angeles, CA, USA

ARTICLE INFO

*Article history:*
Received 11 August 2016
Received in revised form 16 November 2016
Accepted 5 January 2017
Available online 13 January 2017

*Keywords:*
Aging
White matter
Air pollution
Particulate matter
Hippocampus
CA1

ABSTRACT

Traffic-related air pollution (TRAP) is associated with lower cognition and reduced white matter volume in older adults, specifically for particulate matter <2.5-μm diameter ($PM_{2.5}$). Rodents exposed to TRAP have shown microglial activation and neuronal atrophy. We further investigated age differences of TRAP exposure, with focus on hippocampus for neuritic atrophy, white matter degeneration, and microglial activation. Young- and middle-aged mice (3 and 18 months female C57BL/6J) were exposed to nanoscale-PM (nPM, <0.2 μm diameter). Young mice showed selective changes in the hippocampal CA1 region, with neurite atrophy (−25%), decreased MBP (−50%), and increased Iba1 (+50%), with dentate gyrus relatively unaffected. Exposure to nPM of young mice decreased GluA1 protein (−40%) and increased TNFa mRNA (10×). Older controls had age changes approximating nPM effects on young, with no response to nPM, suggesting an age-ceiling effect. The CA1 selective vulnerability in young mice parallels CA1 vulnerability in Alzheimer's disease. We propose that TRAP-associated human cognitive and white matter changes involve hippocampal responses to nPM that begin at younger ages.



## 1. Introduction

Traffic-related air pollution (TRAP) is a ubiquitous environmental toxin, which is associated with poorer cognitive performance in older populations (Power et al., 2011; Ranft et al., 2009; Wellenius et al., 2012; Zeng et al., 2010). The lower cognitive functioning approximates a 2-year advance of normal cognitive decline from aging (Ailshire and Clarke, 2015; Ailshire and Crimmins, 2014; Weuve et al., 2012). Brain structural and cellular changes are less documented. Small decreases of white matter (WM) volume were detected by MRI in older US women of the Women's Health Initiative Memory Study (WHIMS) cohort who resided in zones of high level fine particulate matter ($PM_{2.5}$), with dose exposure in proportion to quartile $PM_{2.5}$ (Chen et al., 2015). Histochemical studies further showed WM microglial activation and blood brain barrier leakage in a small postmortem sample of young adults from a highly polluted Mexican city (Calderón-Garcidueñas et al., 2008, 2011). In several rodent models, TRAP exposure activated microglia (Block and Calderón-Garcidueñas, 2009; Block et al., 2007; Cheng et al., 2016). Effects of aging in animal models of TRAP have received limited study and show divergent age responses. Mumaw et al. (2016), reported increased cerebral cortex microglial reactivity with aging in male C57BL/6J mice ('B6') exposed to TRAP model in vivo.

In view of the potential importance of white matter loss from TRAP exposure in the WHIMS cohort (Chen et al., 2015), we examined the impact of aging on responses to TRAP in white matter and microglia of the dorsal hippocampus in female mice. Neuronal responses were included, because $PM_{2.5}$ exposure of B6 male mice caused selective atrophy of hippocampal CA1 pyramidal neurons (Fonken et al., 2011), and nPM exposure decreased hippocampal CA1 neurite density in female E3FAD mice (Cacciottolo et al., 2017). The selectivity of CA1 neurons to TRAP is relevant to cognitive loss in association with $PM_{2.5}$, because the CA1 pyramidal neurons are the most vulnerable to Alzheimer's disease (AD; Padurariu et al., 2012; Serrano-Pozo et al., 2011).

The present study addresses interactions of age and TRAP by chronically exposing young (3 months) and older (18 months) female B6 mice to nanoscale particulate matter (nPM), a nano-size subfraction of ambient $PM_{2.5}$, which has greater cytotoxicity

* Corresponding author at: USC, Gerontology, 3715 McClintock Ave, Los Angeles, CA 90089-0191, USA. Tel.: +1 (213) 740-1758; fax: +1 (213) 740-0792.
*E-mail address:* cefinch@usc.edu (C.E. Finch).

0197-4580/$ – see front matter © 2017 Elsevier Inc. All rights reserved.
http://dx.doi.org/10.1016/j.neurobiolaging.2017.01.007

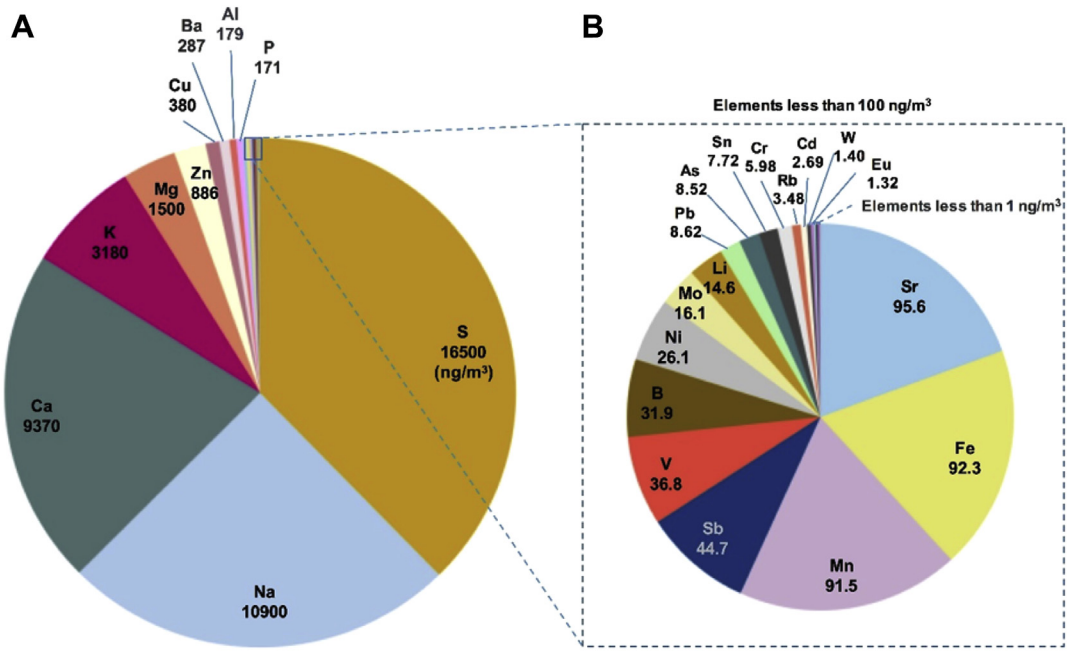


**Fig. 1.** Composition of reaersolized nPM used for exposures. Mass concentration, 342 ± 81 μg/m$^3$; particle number concentration, 1.4 × 10$^5$ ± 9.7 × 10$^3$ particles/cm$^3$. Top inorganic elements are listed in ng/m$^3$. (A). Top 10 elements by concentration. (B). Expanded scale for remaining elements with a concentration >1.0 μg/m$^3$. Abbreviation: nPM, nanoscale particulate matter.

*in vivo and in vitro* than larger PM (Gillespie et al., 2013; Li et al., 2003). In neonatal neuron cultures, nPM inhibited neurite outgrowth via TNFa and TNFR1, and caused growth cone collapse (Cheng et al., 2016). In hippocampal slice cultures nPM caused NMDA-dependent neurotoxicity and nitrosylative stress, with both rescued by NMDA receptor antagonist AP5 (Davis et al., 2013; Morgan et al., 2011).

The age of 18 m at tissue collection demographically approximates a perimenopausal group a decade or more earlier than in the WHIMS cohort. This age also minimizes pathological confounds from tumors and other senescent organ pathology which emerge after 22–24 months (Finch, 2009; Finch and Foster, 1973) in association with exponential increasing mortality (Finch and Pike, 1996).

## 2. Methods

### 2.1. Animals and ethics statement

C57BL/6J female mice, 3 and 18 m were obtained from the NIA Aging Mouse Colony, n = 9 per group. Protocols were approved by the University of Southern California Institutional Animal Care and Use Committee, and animals were maintained under standard conditions according to NIH guidelines.

### 2.2. nPM collection and exposure

Ambient nanoscale particulate matter (nPM; particles with aerodynamic diameters less than 0.18 μm) were collected on a 8 × 10 inch-Zeflour PTFE filters (Pall Life Sciences, Ann Arbor, MI, USA) by a High-Volume Ultrafine Particle Sampler (Misra et al., 2002) at 400 L/min flow rate at the Particle Instrumentation Unit of USC within 150-m downwind of a major freeway (I-110). These aerosols represent a mix of fresh ambient PM mostly from vehicular traffic on this freeway (Ning et al., 2007). Gravimetric mass (nPM mass concentration) was determined from preweighing and postweighing the filters under controlled temperature (22 °C–24 °C) and relative humidity (40%–50%). The filter-deposited dried nPM were eluted by sonication into deionized water, yielding 340 μg/mL. Frozen stocks at 20 °C retain chemical stability for >30 days, including long-lived free radicals (Li et al., 2003; Morgan et al., 2011). Collected nPM has trace endotoxin levels (2.5 EU/mL, which equals approximately 0.3–0.6 ng/mL, by *Limulus* amoebocyte assay), equal to that eluted from filter-collected ambient air. Endotoxin units at the concentration used for cell culture were 0.05–0.08 EU/mL, equivalent to sterile water.

Total elemental composition of the nPM samples was quantified by digestion of a section of the filter-collected nPM using a microwave aided, sealed bomb, mixed acid digestion (nitric acid, hydrofluoric acid and hydrochloric acid). Digests were subsequently analyzed by high resolution inductively coupled plasma sector field mass spectrometry (SF-ICPMS; Herner et al., 2006).

Total nPM mass and number concentrations were 342 ± 49 μg/m$^3$ and 1.4 × 10$^5$ ± 9.7 × 10$^3$ particles/cm$^3$, respectively. The size distribution of the reaerosolized nPM was comparable to typical ambient aerosols, for example, on the 710 Freeway (Ntziachristos et al., 2007). The chemical composition of ions ($NH_4^+$, $NO_3^-$, $SO_4^{2-}$) and water soluble organic compounds was similar to ambient air at the collection site (Morgan et al., 2011). The reaersolized nPM was depleted in insoluble species, including black carbon and polycyclic aromatic hydrocarbons. Fig. 1 displays the average concentrations of inorganic elements in the nPM samples. Nineteen elements were >10 ng/m$^3$ (e.g., copper, Cu, 380 ng/m$^3$), and 29 elements were between 1 and 10 ng/m$^3$ (e.g., iron, Fe, 92.3 ng/m$^3$; Fig. 1A and B, respectively). The organic components of nPM are described in Morgan et al. (2011).

Mice were exposed 5 h/d, 3 d/wk, for 10 weeks (Fig. 2). Collected nPM was reaerosolized, mixed with HEPA-filtered air, and delivered at a constant concentration. Control mice were exposed to only HEPA-filtered air. The reaerosolized nPM exposure stream was assayed for mass concentration by gravimetric analysis of filters parallel to the exposure stream before and after each exposure. The number concentration of the inlet aerosol was

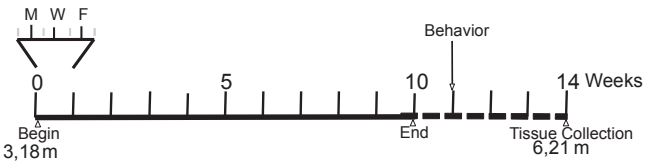


**Fig. 2.** Experimental exposure schedule, showing expanded alternate day intermittent exposure schedule for the initial week; ages of mice at beginning and end of experiment below the timeline.

monitored throughout the exposure period using a condensation particle counter (CPC, TSI Inc.). For the purpose of exposure, mice were transferred from home cages into sealed exposure chambers that allowed adequate ventilation and divided animals to minimize aggression and returned to home cages immediately after exposure.

### 2.3. Weight and behavior

#### 2.3.1. Weight

Mice were weighed before and throughout the exposure. Statistical significance of age and nPM exposure effects was evaluated by 2-way repeated measures ANOVA and Bonferroni post hoc test, and 1-way ANOVA with Tukey post hoc test at the end of exposure.

#### 2.3.2. Novel object recognition (NOR)

Short- and long-term memory were assessed by the NOR test. Mice were tested on a 3-day protocol, to assess short- and long-term memory, and exploratory behavior. On day 1, mice were individually acclimatized to a dimly-lit black Plexiglas cubic box (20 × 20 × 20 cm) for 15 minutes. After 24 hours, mice were returned to the box and exposed to 2 identical novel objects (3.5 × 8 cm), which were affixed to the floor and placed symmetrically at 6 cm from the nearest walls. Mice were placed in a corner, facing the center and at equal distances from the 2 objects. Their start position was rotated and counterbalanced throughout the test. Exploration, defined as sniffing or touching of the 2 objects, was recorded; sitting on the object was not considered exploration. Ninety minutes after the first trial, 1 object was replaced, and the procedure was repeated; 24 hours later, the novel object was replaced with a second novel object, and the trial was repeated to assess long-term memory. The novelty exploration index was calculated by time spent exploring the novel object, divided by time spent exploring the previous object. Statistical analysis for all tests used ANOVA, with Tukey's post hoc test.

#### 2.3.3. Spontaneous alternation of behavior (SAB)

Working memory was assessed by the spontaneous alternation of behavior (SAB) test. The apparatus consisted of 3 equivalent arms (15 × 8 × 10 cm) made of black Plexiglas with equal angles between all arms. Mice were individually placed in 1 arm and allowed to freely explore for 10 minutes. The sequence and entries in each arm were recorded and percent alternation was determined from consecutive entries to the 3 different arms over the total number of transitions.

### 2.4. Histochemistry

Dorsal hippocampus and forceps major of the corpus callosum paired with hippocampal alveus were analyzed by sagittal sections, approximately 1.80 mm from midline (Mouse Brain Atlas, Franklin and Paxinos, 3rd edition) for analysis of subregions CA1 stratum oriens (25 $mm^2$), CA1 stratum radiatum (45 $mm^2$), DG molecular layer (90 $mm^2$), and DG polymorphic layers (15 $mm^2$).

#### 2.4.1. Immunofluorescence

After cardiac saline perfusion, brain hemispheres were immersed in 4% paraformaldehyde overnight; cryoprotected in 30% sucrose; embedded in Optimal Cutting Temperature medium; and sliced sagittally in 18-μm thick sections on a cryostat. Sections were stored at −80 °C. Tissue sections were permeabilized with 1% NP-40 and blocked with 5% bovine serum albumin. Primary antibodies to Iba1 (ionized calcium binding adaptor molecule 1) (1:500, 019−19,741, Wako Pure Chemical Industries, AB839504) or MBP (myelin basic protein, 1:1000, ab40390, Abcam, AB1141521) were added overnight at 4 °C. Immunofluorescence was visualized by Alex Fluor 488 and 594 antibodies (1:400, goat, Molecular Probes).

#### 2.4.2. Silver stain

Slides were defrosted, incubated in 20% silver nitrate for 15 minutes, followed by 20% ammonical silver nitrate for 15 minutes, before developing with a solution of formaldehyde, citric acid, nitric acid, and ammonium hydroxide (de Olmos et al., 1994). Slides were dehydrated and coverslipped with Permount.

#### 2.4.3. Analysis

Using Image J, images were thresholded and quantified for total integrated density. Silver-stained images were skeletonized and filtered to resolve cell bodies and processes. Results were normalized to the average of 3 m controls. Statistical analysis used ANOVA, with Tukey's post hoc test.

### 2.5. Western blots

Dorsal hippocampus of the contralateral hemisphere was microdissected and homogenized by a motor driven pestle on ice in 1× RIPA buffer (Millipore) supplemented with 1-mM PMSF, 1-mM $Na_3VO_2$, 10-mM NaF, phosphatase inhibitor cocktail (Sigma), and Roche Complete Mini EDTA-free protease Inhibitor Cocktail Tablet (Roche). Homogenates were centrifuged 10,000 g × 10 minutes, and supernatants were analyzed by Western blot on Novex NuPAGE 4%−12% Bis-Tris protein gels (Thermo Scientific). Membranes were washed with phosphate-buffered saline with 0.05% tween-20 and blocked with 5% BSA for 1 hour at room temperature. Primary incubation was overnight at 4 °C for glutamatergic receptor protein subunits GluA1 (Abcam), GluA2 (Millipore), NR2A (Millipore), NR2B (Millipore), and other synaptic proteins (Sigma) at 1:1000 overnight and followed by secondary antibodies (1:10,000) conjugated with IRDye 800 (mouse, LI-COR Biosciences) or IRDye 680 (rabbit, LI-COR Biosciences) for 1 hour. Protein bands were quantified by Qdyssey V3.0 software (LI-COR Biosciences).

### 2.6. q-PCR

Hippocampal tissue was microdissected and homogenized by motor driven pestle in TriReagent (Sigma) and 1-bromo-3-chloropropane (Sigma). cDNA was reverse transcribed (Promega) for q-PCR with Taq Master Mix (Biopioneer). Primers used were *TNFa* (forward: CGTCAGCCGATTTGCTATCT; reverse: CGGACTCCGCAAAGTCTAAG), *TNFR1* (forward: TGCCTCTGGTTATCTTCCTA; reverse: GGGGCTTAGTAACAATTCCT), and *GAPDH* (forward: CCAATGTGTCCGTCGTGGATCT; reverse: GTTGAAGTCGCAGGAGACAACC). Q-PCR was quantified by delta-delta-CT.

## 3. Results

Female C57BL/6J mice of specified ages were exposed to 150 hours of nPM during 10 weeks. Mice were behaviorally tested before analysis of brains by histochemistry and for protein and RNA.

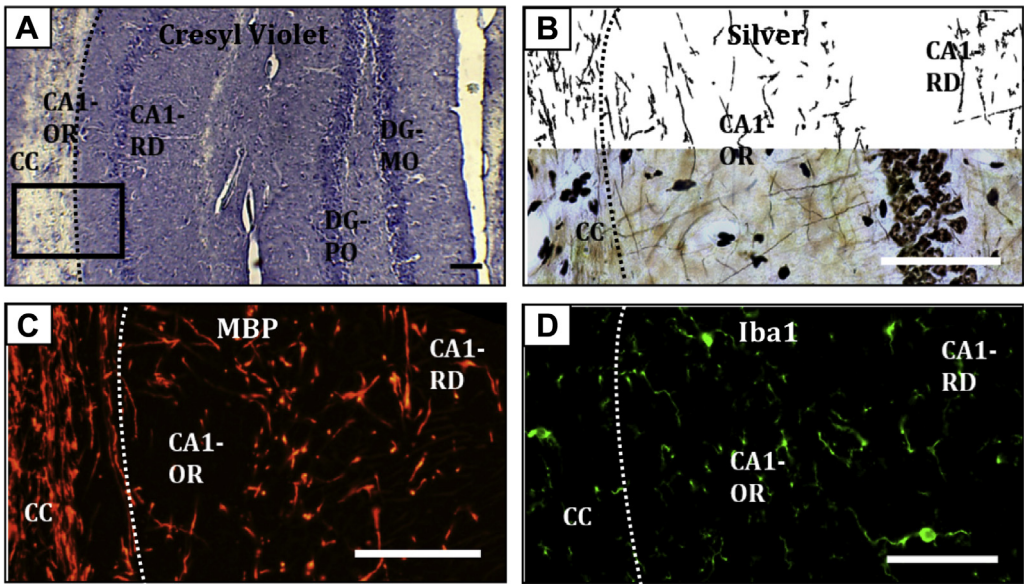


**Fig. 3.** Histochemistry illustrating regions and stains. (A), Cresyl violet stain, corpus callosum (CC), and dorsal hippocampus: CA1 subfields stratum oriens (approximate area of analysis 25 $mm^2$) and stratum radiatum (45 $mm^2$), dentate gyrus (DG) subfields molecular layer (90 $mm^2$), and polymorphic layer (15 $mm^2$). Black box outlines the regions shown in other panels. (B) Silver histochemistry: bottom panel, initial microscopic image; top, skeletonized and filtered to exclude cell bodies. (C) Myelin basic protein; (D) Iba1. Scale bar, 100 μm. (For interpretation of the references to color in this figure legend, the reader is referred to the Web version of this article.)

### 3.1. Histochemistry

The dorsal hippocampus and corpus callosum, including the alveus, were examined for neuronal morphological changes, white matter myelin basic protein (MBP), and microglial activation. Fig. 3 show illustrative images. Age differences are summarized in Table 1; nPM responses of the young, Table 2. The mouse age is shown at the beginning of the 10 weeks exposure.

#### 3.1.1. Neurites

Silver staining of neurites showed effects of age and nPM, with no change in perikarya. Controls showed 25% decrease in CA1 neurite area with age (18 m vs 3 m), whereas dentate gyrus (DG) neurites did not show age change (Fig. 4, ANOVA $p < 0.05$). For nPM exposure, only the young mice responded, with 25% fewer neuritic processes in the CA1 stratum oriens and stratum radiatum (Fig. 4A and B, ANOVA $p < 0.05$). nPM had no effect on CA3 or DG neurite areas in either age group (Fig. 4C and D). Perikaryal staining did not change with age or exposure in these regions (Supplementary Fig. 1).

#### 3.1.2. White matter

In controls, MBP was decreased in older mice in CA1 stratum oriens (−50%), and the DG polymorphic layer (−45%; Fig. 5A and C, ANOVA $p < 0.05$). For nPM exposure, only young mice responded, with 45% decreased MBP in the CA1 stratum oriens (Fig. 5A, ANOVA $p < 0.05$). Exposure did not alter polymorphic or molecular layers of the DG (Fig. 5C and D), or corpus callosum (forceps major) and hippocampal alveus (Fig. 5E). Older nPM exposed mice showed no further decrease in MBP.

#### 3.1.3. Microglial activation

Iba1 immunostaining, a marker for microglial activation, showed +35% age increase in controls (Fig. 6A, $p < 0.05$, 2-tailed $t$ test). nPM exposure increased Iba1 in young mice by +50% in CA1 stratum oriens (Fig. 6A; ANOVA $p < 0.05$), and by +50% in DG polymorphic layer (Fig. 6C, ANOVA $p < 0.05$). Exposure to nPM did not alter Iba1 in CA1 stratum radiatum, DG molecular layer, corpus callosum, and alveus (Fig. 6B, D, and E).

### 3.2. Protein and RNA by Western blot and q-PCR

Glutamatergic receptor protein subunits in whole hippocampal extracts showed selective changes by Western blots. We focused on AMPA receptors (GluA1 and GluA2), which were selectively vulnerable to nPM in young male mice, whereas NMDA subunits were not affected (Morgan et al., 2011). In nonexposed controls,

**Table 1**
Summary of age differences in control mice, not nPM exposed

| Age differences | | | |
|---|---|---|---|
| Region | Neurites | Myelin | Microglial activation |
| CA1 | | | |
| Oriens | −25% | −50% | +35% |
| Radiatum | 0 | 0 | 0 |
| DG | | | |
| Polymorph | 0 | −45% | 0 |
| Molecular | 0 | 0 | 0 |
| Corpus callosum | NA | 0 | 0 |

Summary of age differences in control mice (Figs. 4–6). 0, no change, “Inc” denotes an increase versus young control, “Dec”, a decrease versus young control, and NA, not measured.

**Table 2**
Summary of treatment differences in young animals

| Treatment differences | | | |
|---|---|---|---|
| Region | Neurites | Myelin | Microglial activation |
| CA1 | | | |
| Oriens | −25% | −45% | +50% |
| Radiatum | −25% | 0 | 0 |
| DG | | | |
| Polymorph | 0 | 0 | +50% |
| Molecular | 0 | 0 | 0 |
| Corpus Callosum | NA | 0 | 0 |

CA1-cornus ammonis 1, DG-dentate gyrus.
Values are versus young control air mice. 0 denotes no change, “Inc” denotes increase, “Dec” shows a decrease, and NA means not measured.

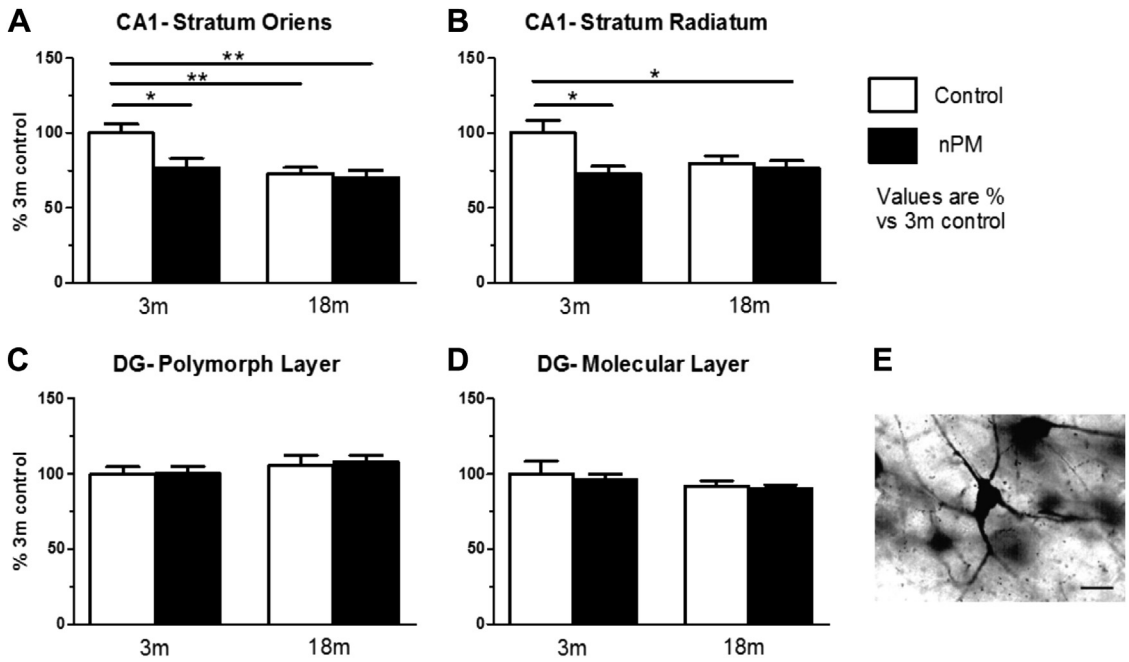


**Fig. 4.** Hippocampus neurite area as total silver-stained area per field (See Fig. 3). (A). Stratum oriens of CA1. nPM exposure in 3m mice decreased processes by 25% ($p < 0.05$, ANOVA), 18m animals had equivalent decrease ($p < 0.05$, ANOVA). No response to nPM in 18m mice. (B). Stratum radiatum of CA1. nPM exposure decreased processes by 25% ($p < 0.05$, ANOVA). No baseline age changes. (C). Polymorphic layer of the DG. No change observed. (D). Molecular layer of the DG. No change observed. (E) Example of silver-stained CA1 stratum radiatum neuron. Mean +/− SEM; $*p < 0.05$, $**p < 0.01$; N = 9 per treatment. Scale bar 25 μm. Abbreviation: SEM, standard error of the mean.

GluA1 protein was decreased −50% by age alone (Fig. 7A, ANOVA $p < 0.05$). Only young mice responded to nPM with −50% decrease in GluA1. Cortical GluA1 protein did not differ by age. Three other subunits did not differ by age or respond to nPM: GluR2, NR2A, NR2B (Fig. 7B, C, and D). No change was observed in phosphorylation of GluA1 at S845 or S831, or of NR2B at S1303 by age or nPM.

TNFa mRNA responded to nPM with major 10-fold increase in young mice (Fig. 7A). Older mice had highly variable TNFa which reduced significance of possible age increase (Fig. 7E, *t*-test $p = 0.002$). TNFR1 mRNA showed no change by age or treatment (Fig. 7F).

### 3.3. Body weight and behavior

#### 3.3.1. Body weight

All groups lost weight during the first 3 weeks of exposure (Fig. 8; $p < 0.01$, 2-way ANOVA), presumably due to handling and noise stress. Young control and exposed mice, as well as older controls, regained their initial weight by the end of the 10-week exposure. In contrast, older mice did not recover weight loss during the exposure (Fig. 8; 1-way ANOVA, $p < 0.05$), but by 4 weeks after exposure had regained the lost weight. Young mice, both nPM and control, which maintained weight throughout exposure, gained weight after conclusion of the exposure (Fig. 8; 2-way ANOVA, $p < 0.0001$).

#### 3.3.2. Cognition and activity

No memory deficits were observed for age or for nPM exposure by NOR (Fig. 9B) or SAB (Fig. 10B). However, nPM exposure did decrease exploratory activity in both tests. The novel object recognition (NOR) test for short- and long-term memory showed 30% less exploration for older mice exposed to nPM versus controls (Fig. 9A; ANOVA $p < 0.01$). In the spontaneous alternation of behavior test for short-term memory, the total arm entries were decreased in both young and older mice, versus age-matched controls (Fig. 10A, 2-way ANOVA, $p < 0.05$). Individual weight loss was correlated with locomotor activity change for older exposed mice (Fig. 11; r = 0.51), with the heavier exploring more.

## 4. Discussion

Young female mice (3 m) given 10 weeks of intermittent exposure to nPM from ambient urban traffic emissions showed changes resembling baseline aging changes of hippocampal CA1 subregion-specific decrease of MBP in WM and atrophy of CA1 neurites, together with microglial activation. Young nPM exposed mice also showed decreased hippocampus GluA1 protein and increased TNFa mRNA.

The reduction in myelin basic protein (MBP) is the first experimental evidence of WM alteration by air pollution exposure. These findings extend observed correlations of WM volume loss with ambient PM2.5 in older woman of the WHIMS cohort (Chen et al., 2015), which could be in part responsible for the decline in cognitive performance from TRAP exposure in older populations (Ranft et al., 2009; Wellenius et al., 2012; Zeng et al., 2010), approximating 2 years of normal cognitive aging (Ailshire and Clarke, 2015; Ailshire and Crimmins, 2014). This change could begin at young ages, evidenced from WM microglial activation in a small post-mortem sample from a highly polluted Mexican city (Calderón-Garcidueñas et al., 2008, 2011). Future studies will analyze WM for MBP isoforms and other WM proteins, as well as fiber density.

### 4.1. Aging and response to nPM

Responses to nPM were diminished by aging. In young adult mice, the nPM exposure decreased MBP levels and neurites, and increased microglial activation in the hippocampal CA1 subfields. The older controls (nonexposed, 18 m.) had 25% lower CA1 neurite density and 50% less MBP, with a trend toward the microglial activation. Older controls also showed decreased GluA1 and

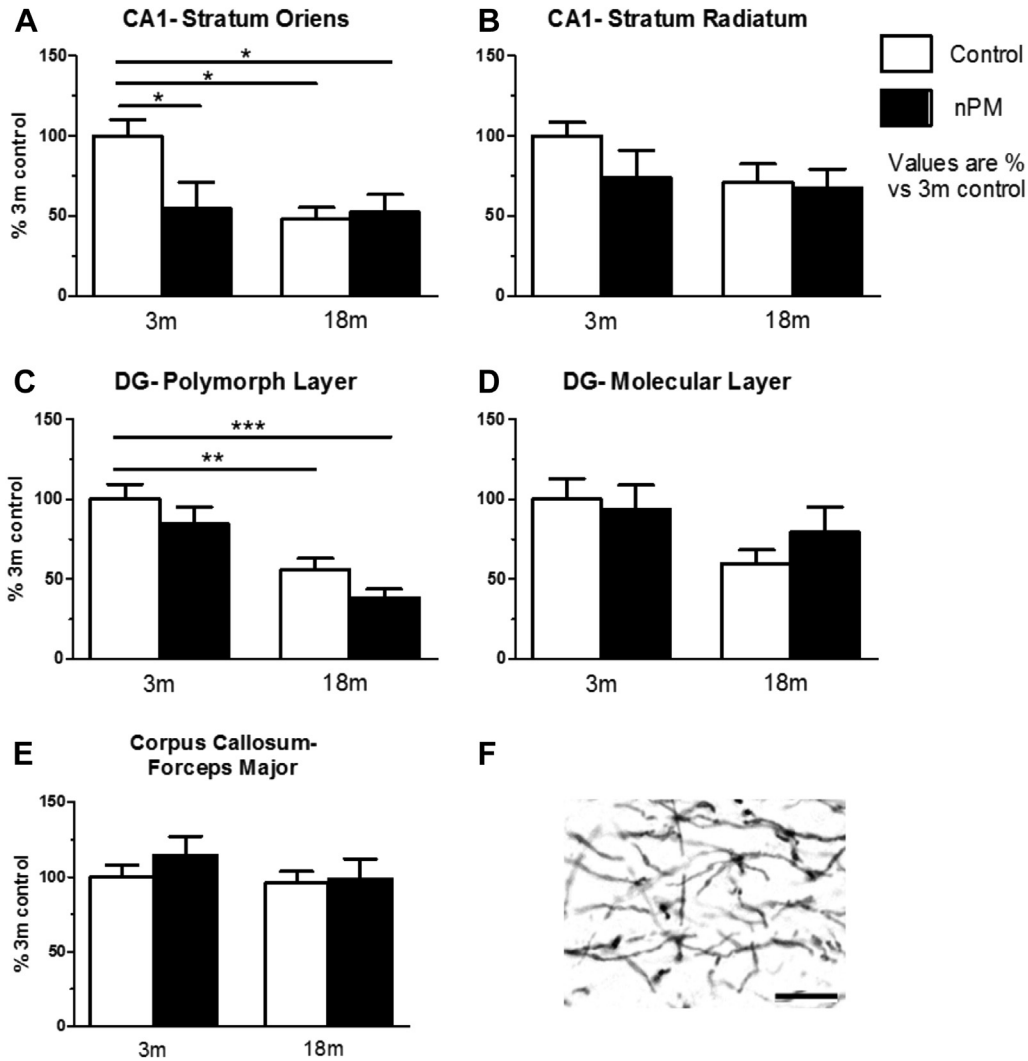


**Fig. 5.** White matter immunohistochemistry for myelin basic protein in hippocampus and corpus callosum (See Fig. 3). (A). Stratum oriens of CA1. nPM exposure in 3m mice decreased MBP by 50% ($p < 0.05$, ANOVA). Of all, 18m animals had equivalent decrease ($p < 0.05$, ANOVA). No response to nPM in 18m mice. (B). Stratum radiatum of CA1. No change observed by age or nPM. (C). Polymorphic layer of the dentate gyrus (DG). No response to nPM in 3m or 18m mice. Baseline age change of 50% ($p < 0.05$, ANOVA). (D). Molecular layer of the DG. No change observed. (E) Forceps major of the corpus callosum. No change observed. (F). Example of MBP stained myelin in CA1 stratum radiatum. Mean +/− SEM; $^{*}p < 0.05$, $^{**}p < 0.01$, $^{***}p < 0.001$; N = 9 per treatment. Scale bar 10 μm. Abbreviation: SEM, standard error of the mean.

increased TNFa. However, the older mice did not respond to nPM with further atrophic brain changes. The diminished response of older mice to nPM was anticipated by the smaller kainate excitotoxic lesions of 20- and 24-m-old aging male rats versus 3 m (Kesslak et al., 1995). The mechanisms behind the age-ceiling effect of hippocampus to nPM could involve an age-related loss of glutamate receptors (Fig. 7A; Magnusson and Cotman, 1993) and age-related insensitivity to excitotoxins in the CA1 (Kerr et al., 2002), reported for older male rats. Our results support this hypothesis, with baseline decreased GluA1 in older mice. These findings also extend findings that 18-m-old male C57BL/6J mice did not respond to nPM with induction of phase II electrophile responses in cerebellum, lung, and liver (Zhang et al., 2012).

Older mice showed nPM vulnerability in weight loss and behavioral activity. Older exposed mice lost more body weight during nPM exposure, and unlike the young and the older controls, did not recover weight until 1 month after the exposure. Older nPM exposed mice also had reduced exploration in the novel object recognition test (30% reduction). Both young and older exposed mice showed less alternations in the spontaneous alternation of behavior test (20% reduction). Moreover, individual weight loss was correlated with locomotor activity change for older exposed mice, with heavier animals exploring more.

The tests of short-term and long-term memory did not show effects of age or nPM. The NOR test measures declarative memory but does not specifically resolve pattern completion. Memory tests that delineate between mechanisms of recall (Fanselow, 1990; Matus-Amat et al., 2004) could be considered in future studies. Because the NOR is not directly hippocampal dependent, future studies could include contextual object recognition tests which are hippocampal dependent, for example, Novel Object In Context (NOIC [Balderas et al., 2008]). A comprehensive brain regional analysis is needed to identify the vulnerability of neuronal pathways to ambient pollutants across the lifespan. This effort is justified by the global impact of air pollution on health and mortality, which the WHO ranks in top 20 leading risk factors for mortality (WHO, 2009).

### 4.2. Young mice nPM responses

Contrary to the absence of nPM effects on memory, we found CA1-specific neurite atrophy in young mice. The regional

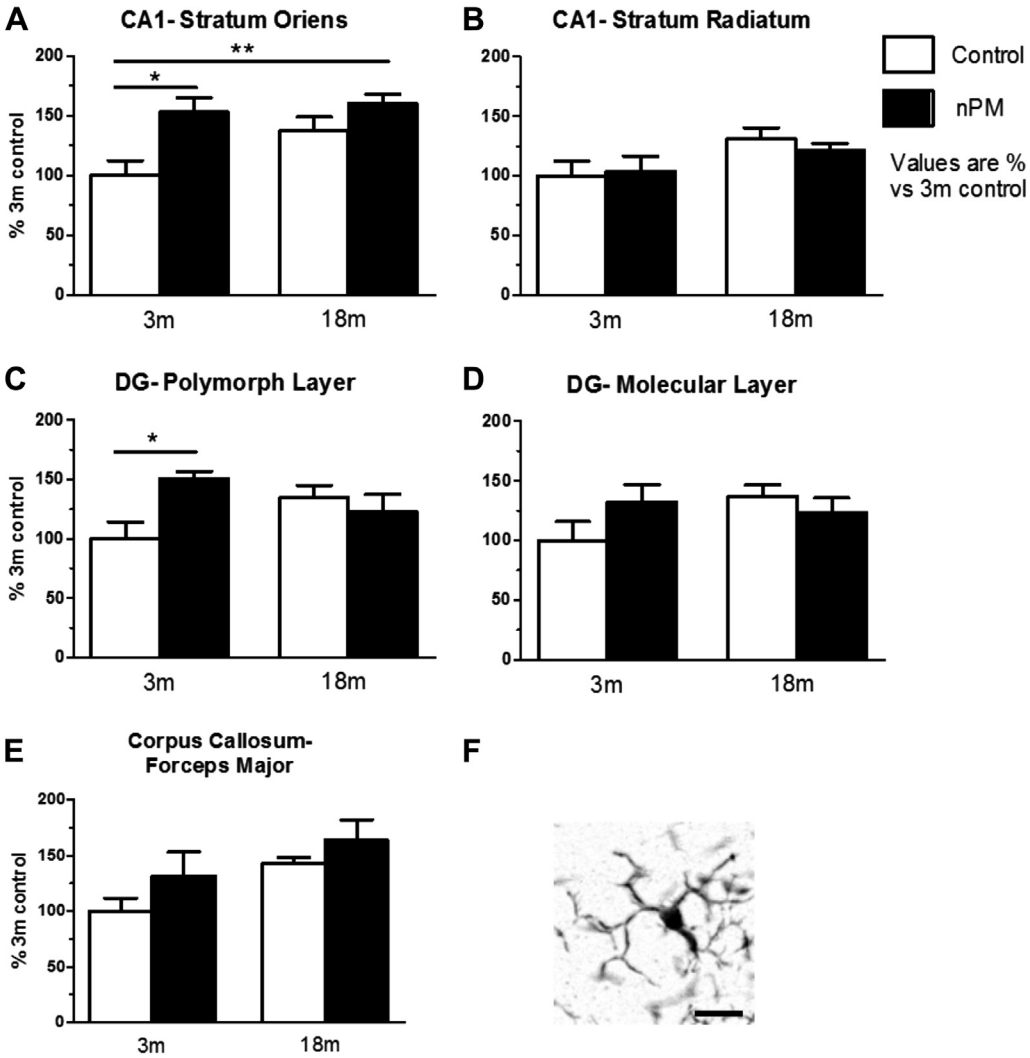


**Fig. 6.** Microglial activation, measured by Iba1 immunohistochemistry (IHC), in regions of the hippocampus and corpus callosum (See Fig. 3). (A). Stratum oriens of CA1. nPM exposure in 3m mice increased Iba1 by 50% ($p < 0.05$, ANOVA). Older control mice showed a trend toward decrease, with no change observed by ANOVA, but $p < 0.05$ by 2-tailed $t$ test. No response to nPM in 18m mice. (B). Stratum radiatum of CA1. No changes observed. (C). Polymorphic layer of the dentate gyrus (DG). nPM exposure in 3m mice increased Iba1 by 50% ($p < 0.05$, ANOVA). No baseline age changes or response to nPM in 18m mice observed. (D). Molecular layer of the DG. No changes observed. (E). Microglial expression in the corpus callosum, no change. (F). Example of Iba1-stained microglial cell from CA1 stratum radiatum. Mean +/− SEM; $^{*}p < 0.05$, $^{**}p < 0.01$; N = 9 per treatment. Scale bar 10 μm.

vulnerability of hippocampal neurons gives a precedent for further inquiry. The CA1 stratum oriens responded most to nPM exposure, with a 25% neurite atrophy, 50% reduction in MBP, and 50% increase in Iba1. The stratum radiatum showed changes only in neurites, whereas white matter and Iba1 remaining unchanged. These regions, though adjacent, differ in vascularization, cell population, and connectivity, which could explain the divergent responses to nPM. The stratum oriens is more densely vascularized than the stratum radiatum (Duvernoy et al., 2013; Grivas et al., 2003) and has different connectivity. For example, the entorhinal cortex projections to the stratum oriens are denser than to the stratum radiatum, whereas CA3 sends projections to both strata, but with more projections to the radiatum, via the Schaffer collaterals. The MBP and microglial changes in response to nPM were observed only in the stratum oriens, which predicts LTP impairments to nPM in the oriens. The data for 3-month mice in Fig. 3A, B, D and E are also represented in a different format in Fig. 3C and D of Cacciottolo et al. (2017).

The selective atrophy of CA1 neurites in young C57BL/6J female mice in our study confirms the Golgi analysis of Fonken et al., 2011, for young male B6 mice; in both studies, the DG neurites were unchanged. The silver staining of 18-μm sections could not resolve dendritic spines or other neuronal subprocesses. The differential CA1 vulnerability to 2 models of TRAP exposure closely matches the CA1 vulnerability in AD, wherein the CA1 neurons undergo earlier and greater degeneration than the DG (Padurariu et al., 2012; Serrano-Pozo et al., 2011). This regional vulnerability has important implications for the cognitive consequences of TRAP exposure. The CA1 is integral in spatial memory (Tsien et al., 1996), consistent with the poorer performance on the Barnes maze of $PM_{2.5}$-exposed mice (Fonken et al., 2011). The CA1 also mediates object recognition, specifically pattern completion recall, based on familiar cues, and is mediated by the CA3/CA1 pathway (Leal and Yassa, 2015).

Effect of nPM on glutamate receptors in young mice was selective to GluA1 AMPA receptors, with no change in GluA2, or the NMDA receptors NR2A and NR2B. This selectivity was observed in male mice with the same nPM exposure (Morgan et al., 2011). Neonatal hippocampal slice experiments also show acute glutamatergic pathway responses to nPM: the greater CA1 vulnerability

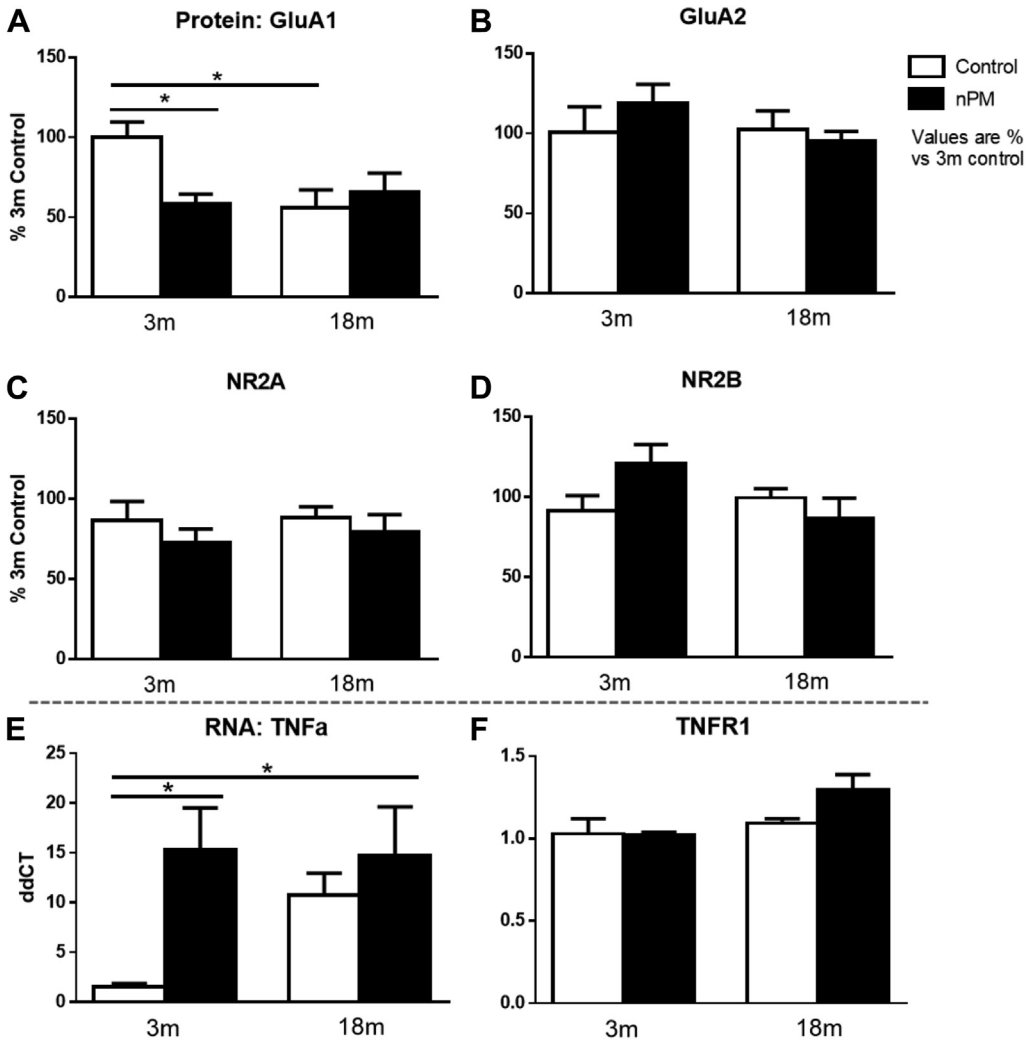


**Fig. 7.** Protein concentration of glutamate receptor subunits from hippocampal lysates. (A). GluA1 protein was decreased 50% in the 3m mice by nPM exposure ($p < 0.05$, ANOVA). Baseline age decrease of 50% was observed ($p < 0.05$, ANOVA), with no effect of nPM in older mice. (B). GluA2 protein showed no change by age or treatment. (C) NR2A showed no change by age or treatment. (D). NR2B showed no change. (E). TNFa mRNA in the hippocampus, by q-PCR. nPM exposure increased TNFa mRNA in young mice by 10× ($p < 0.05$, ANOVA). Nonexposed controls showed a trend for age increase that was not significant because of individual variability. (F). TNFR1 mRNA, no change by age or treatment. Dotted line separates protein and RNA results. Mean +/− SEM; *$p < 0.05$; N = 9 per treatment. Abbreviation: SEM, standard error of mean.

and induction of NO and nitrosylation were attenuated by the NMDA receptor antagonist AP5 (Davis et al., 2013).

The neurite atrophy with decreased length could be TNFa dependent. In vitro nPM exposure reduced neurite outgrowth in a TNFa/TNFR1-dependent manner (Cheng et al., 2016). Hippocampal TNFa mRNA was increased 10× in by nPM exposure in the present studies. In vitro blocking TNFa by siRNA or immunoneutralization was able to rescue neurite growth, as was blocking TNFR1 by anti-TNFR1 peptide (Cheng et al., 2016). We saw no change in TNFR1 mRNA, corroborating findings on the olfactory neurepithelium (Cheng et al., 2016).

### 4.3. Exposure composition

The exposure concentrations used here are roughly equal in overall particle numbers to ambient on-road concentrations (Ntziachristos et al., 2007). The overall delivered dose over the 10-week exposure protocol is roughly equivalent to 1 year of human exposure to freeway levels of nPM. The nPM used here is generalizable to other cities, as it is mostly derived from automobile traffic. Despite the overall low levels of metals in ambient nPM, redox-active elements such as Cu, Cr, Fe, Mn, and Ni have been attributed to

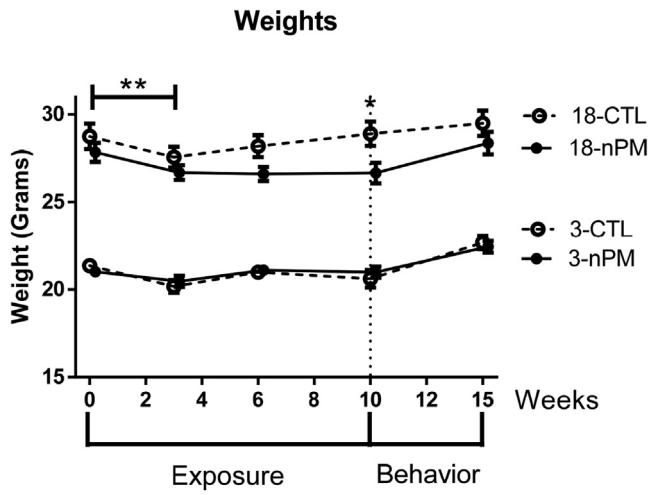


**Fig. 8.** Body weight throughout exposure and 1 m post exposure. All groups showed initial weight loss ($p < 0.01$, 2-way ANOVA). All young mice and older controls recovered weight during the exposure, unlike older exposed mice; difference post exposure ($p < 0.05$, 1-way ANOVA). Older exposed mice recovered weight 1 m post exposure. Mean +/− SEM; *$p < 0.05$, **$p < 0.01$; N = 9 per group. Abbreviation: SEM, standard error of mean.

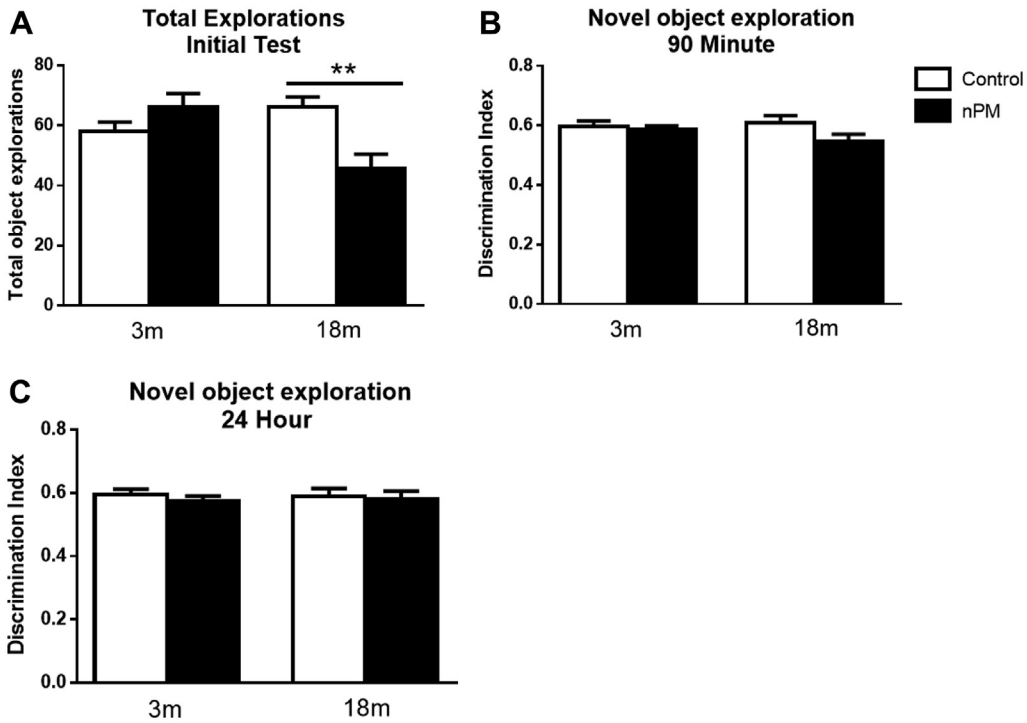


**Fig. 9.** Novel Object Recognition (NOR) test, activity, and discrimination index. (A). Total number of explorations during the initial test. Older nPM exposed mice had reduced exploratory activity ($p < 0.01$, 1-way ANOVA). (B). Discrimination index (exploration of novel object divided by total exploration) for the 90-min post-test (short-term memory). (C). Discrimination index for the 24-h post-test (long-term memory). Mean +/− SEM; $^{**}p < 0.01$; N = 9 per treatment. Abbreviation: SEM, standard error of the mean.

adverse health outcomes (Molinelli et al., 2002; Oller, 2002; Wise et al., 2002). Prior studies in the Los Angeles basin and elsewhere have indicated that these metals in the submicron size ranges are mostly emitted from motor vehicles, including tailpipe emissions, brake wear, tire wear, and resuspended road dust, in addition to combustion products (Saffari et al., 2013; Schauer et al., 2006).

### 4.4. Potential mechanisms

The transport of nPM and other TRAP components into the brain is unresolved and includes at least 2 routes, “nose-to-brain” and “lung-to-brain”. Other ultrafine PM (radiolabelled carbon and manganese) can be translocated to the brain from the olfactory neurons in the nasal epithelium into the olfactory bulb but also to other brain regions (Elder et al., 2006; Oberdorster et al., 2004). We recently showed rapid inflammatory responses in the olfactory bulb to inhaled nPM (Cheng et al., 2016). In addition, Mumaw et al. (2016), showed evidence for a lung-to-brain route in response to ozone which did not involve TNFa or other cytokines. Nonetheless, TRAP exposure can increase blood TNFa in humans (Delfino et al., 2009) and mice (Li et al., 2013; van Eeden et al., 2001). Elucidating specific chemical mechanisms in responses to nPM and other TRAP components is complicated by their extreme chemical heterogeneity (Liu et al., 2016; Morgan et al., 2011). Besides direct “nose-to-brain” passage of inhaled air particulates, radiolabeled ultrafine carbon PM rapidly reached the cerebellum at about the same time as the olfactory bulb (Oberdorster et al., 2004), suggesting other routes into the brain. The possibility of systemic effects of inhaled TRAP are consistent with the broad brain regional responses to TRAP inhalation, which include cerebellum (Cheng et al., 2016; Zhang et al., 2012) and other regions that are multiple synapses away from olfactory input.

The cellular mechanisms of nPM induced neurodegeneration could be mediated by chronic microglial activation, which produces

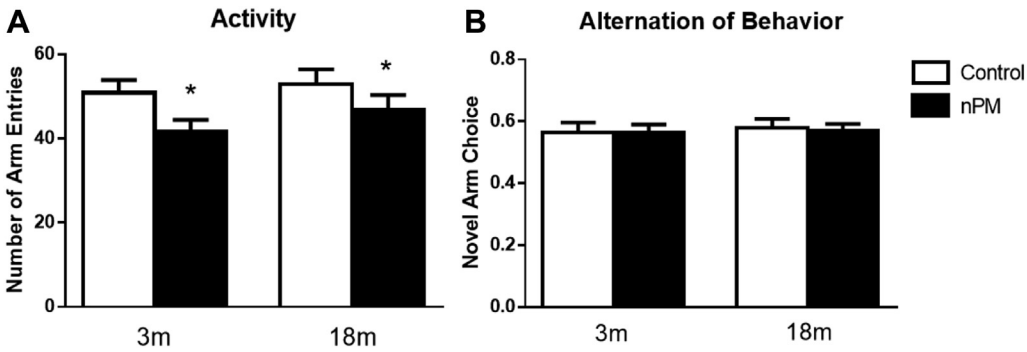


**Fig. 10.** Spontaneous Alternation of Behavior (SAB) test. (A). Total number of alternations between the 3 arms. Both ages showed effect of nPM ($p < 0.05$, 2-way ANOVA. (B). Alternation of behavior (ratio of optimal arm choices). Mean +/− SEM; $^{*}p < 0.05$; N = 9 per treatment. Abbreviation: SEM, standard error of the mean.

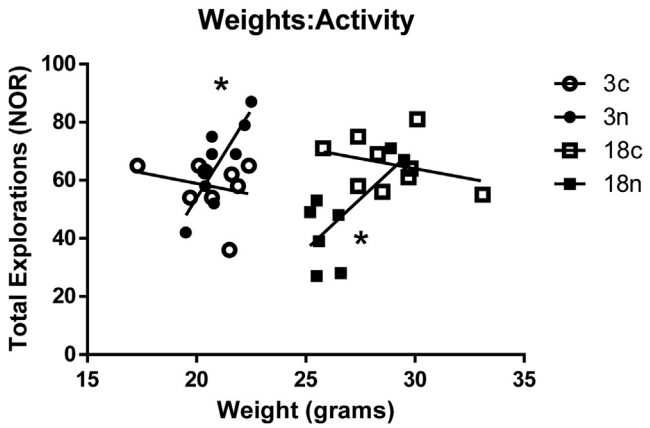


**Fig. 11.** Correlations of body weight at the end of nPM exposure versus total number of explorations in the initial NOR test. Both ages showed effect of nPM (r = 0.5076), $^{*}p < 0.05$.

both extracellular reactive oxygen species and neurotoxic factors (Block et al., 2007; Davis et al., 2013; Mumaw et al., 2016). LPS-based microglial activation shows neuronal loss in microglial rich brain regions (Qin et al., 2007) and causes reduced neuronal processes in the CA1 (Richwine et al., 2008). Exposure to nPM shows neuroinflammatory effects including induced inflammatory cytokines seen in the cerebral cortex (Morgan et al., 2011) and increased phase II response genes in the cerebellum (Zhang et al., 2012). nPM treatment of mixed glial cultures increased IL-1a and TNFa with dose dependence (Morgan et al., 2011). The present study extends these results of neuroinflammation in the CA1 and dentate gyrus, and subregional specificity of the nPM response.

## 5. Conclusion

Shown here, nPM leads to hippocampal neurite atrophy and decreased white matter MBP. The regional specificity to the CA1 predicts a degradation of CA1 functions in human populations exposed to high levels of air pollution, which underlie accelerated cognitive impairments. Future imaging studies of WHIMS and other well defined cohorts may resolve earlier stages of neurodegenerative responses to TRAP and their relationship to AD risk.

## Disclosure statement

The authors have no conflicts of interest to disclose.

## Acknowledgements

The authors thank Prof. Joshua Millstein for statistical advice; and Prof. Jiu Chiuan Chen for his careful review of the manuscript. This work was supported by the National Institutes of Aging (T32AG0037, R21 AG-040753, R21 AG-050201).

## Appendix A. Supplementary data

Supplementary data associated with this article can be found, in the online version, at http://dx.doi.org/10.1016/j.neurobiolaging.2017.01.007.

## References

Ailshire, J.A., Clarke, P., 2015. Fine particulate matter air pollution and cognitive function among U.S. older adults. J. Gerontol. B Psychol. Sci. Soc. Sci. 70, 322–328.

Ailshire, J.A., Crimmins, E.M., 2014. Fine particulate matter air pollution and cognitive function among older US adults. Am. J. Epidemiol. 180, 359–366.

Balderas, I., Rodriguez-Ortiz, C.J., Salgado-Tonda, P., Chavez-Hurtado, J., McGaugh, J.L., Bermudez-Rattoni, F., 2008. The consolidation of object and context recognition memory involve different regions of the temporal lobe. Learn Mem. 15, 618–624.

Block, M.L., Calderón-Garcidueñas, L., 2009. Air pollution: mechanisms of neuroinflammation and CNS disease. Trends Neurosci. 32, 506–516.

Block, M.L., Zecca, L., Hong, J.S., 2007. Microglia-mediated neurotoxicity: uncovering the molecular mechanisms. Nat. Rev. Neurosci. 8, 57–69.

Cacciottolo, M., Wang, X., Driscoll, I., Woodward, N., Saffari, A., Reyes, J., Serre, M.L., Vizuete, W., Sioutas, C., Morgan, T.E., Gatz, M., Chui, H.C., Shumaker, S.A., Resnick, S.M., Espeland, M.A., Finch, C.E., Chen, J.C., 2017. Particulate air pollutants, APOE alleles, and their contributions to cognitive impairment in older women and to amyloidogenesis in experimental models. Transl Psychiatry 7 e1022.

Calderón-Garcidueñas, L., Engle, R., Mora-Tiscareño, A., Styner, M., Gómez-Garza, G., Zhu, H., Jewells, V., Torres-Jardón, R., Romero, L., Monroy-Acosta, M.E., Bryant, C., González-González, L.O., Medina-Cortina, H., D'Angiulli, A., 2011. Exposure to severe urban air pollution influences cognitive outcomes, brain volume and systemic inflammation in clinically healthy children. Brain Cogn. 77, 345–355.

Calderón-Garcidueñas, L., Solt, A.C., Henríquez-Roldán, C., Torres-Jardón, R., Nuse, B., Herritt, L., Villarreal-Calderón, R., Osnaya, N., Stone, I., García, R., Brooks, D.M., González-Maciel, A., Reynoso-Robles, R., Delgado-Chávez, R., Reed, W., 2008. Long-term air pollution exposure is associated with neuroinflammation, an altered innate immune response, disruption of the blood-brain barrier, ultrafine particulate deposition, and accumulation of amyloid beta-42 and alpha-synuclein in children and young adults. Toxicol. Pathol. 36, 289–310.

Chen, J.C., Wang, X., Wellenius, G.A., Serre, M.L., Driscoll, I., Casanova, R., McArdle, J.J., Manson, J.E., Chui, H.C., Espeland, M.A., 2015. Ambient air pollution and neurotoxicity on brain structure: evidence from women's health initiative memory study. Ann. Neurol. 78, 466–476.

Cheng, H., Saffari, A., Sioutas, C., Forman, H.J., Morgan, T.E., Finch, C.E., 2016. Nanoscale particulate matter from urban traffic rapidly induces oxidative stress and inflammation in olfactory epithelium with concomitant effects on brain. Environ. Health Perspect. 124, 1537–1546.

Davis, D.A., Akopian, G., Walsh, J.P., Sioutas, C., Morgan, T.E., Finch, C.E., 2013. Urban air pollutants reduce synaptic function of CA1 neurons via an NMDA/NO pathway in vitro. J. Neurochem. 127, 509–519.

de Olmos, J.S., Beltramino, C.A., de Olmos de Lorenzo, S., 1994. Use of an amino-cupric-silver technique for the detection of early and semi acute neuronal degeneration caused by neurotoxicants, hypoxia, and physical trauma. Neurotoxicology and teratology 16, 545–561.

Delfino, R.J., Staimer, N., Tjoa, T., Gillen, D.L., Polidori, A., Arhami, M., Kleinman, M.T., Vaziri, N.D., Longhurst, J., Sioutas, C., 2009. Air pollution exposures and circulating biomarkers of effect in a susceptible population: clues to potential causal component mixtures and mechanisms. Environ. Health Perspect. 117, 1232–1238.

Duvernoy, Henri M., Cattin, Francoise, Risold, Pierre-Yves, Duvernoy, H.M., Cattin, F., Risold, P., 2013. The Human Hippocampus- Functional Anatomy, Vascularization, and Serial Sections with MRI. Springer, New York.

Elder, A., Gelein, R., Silva, V., Feikert, T., Opanashuk, L., Carter, J., Potter, R., Maynard, A., Ito, Y., Finkelstein, J., Oberdörster, G., 2006. Translocation of inhaled ultrafine manganese oxide particles to the central nervous system. Environ. Health Perspect. 114, 1172–1178.

Fanselow, M.S., 1990. Factors governing one-trial contextual conditioning. Anim. Learn. Behav. 18, 264–270.

Finch, C.E., 2009. The neurobiology of middle-age has arrived. Neurobiol. Aging 30, 515–520 discussion 530–3.

Finch, C.E., Foster, J.R., 1973. Hematologic and serum electrolyte values of the C57BL-6J male mouse in maturity and senescence. Lab Anim. Sci. 23, 339–349.

Finch, C.E., Pike, M.C., 1996. Maximum life span predictions from the Gompertz mortality model. J. Gerontol. A. Biol. Sci. Med. Sci. 51, B183–B194.

Fonken, L.K., Xu, X., Weil, Z.M., Chen, G., Sun, Q., Rajagopalan, S., Nelson, R.J., 2011. Air pollution impairs cognition, provokes depressive-like behaviors and alters hippocampal cytokine expression and morphology. Mol. Psychiatry 16, 987–995.

Gillespie, P., Tajuba, J., Lippmann, M., Chen, L.C., Veronesi, B., 2013. Particulate matter neurotoxicity in culture is size-dependent. Neurotoxicology 36, 112–117.

Grivas, I., Michaloudi, H., Batzios, Ch, Chiotelli, M., Papatheodoropoulos, C., Kostopoulos, G., Papadopoulos, G.C., 2003. Vascular network of the rat hippocampus is not homogeneous along the septotemporal axis. Brain Res. 971, 245–249.

Herner, J.D., Green, P.G., Kleeman, M.J., 2006. Measuring the trace elemental composition of size-resolved airborne particles. Environ. Sci. Technol. 40, 1925–1933.

Kerr, D.S., Razak, A., Crawford, N., 2002. Age-related changes in tolerance to the marine algal excitotoxin domoic acid. Neuropharmacology 43, 357–366.

Kesslak, J.P., Yuan, D., Neeper, S., Cotman, C.W., 1995. Vulnerability of the hippocampus to kainate excitotoxicity in the aged, mature and young adult rat. Neurosci. Lett. 188, 117–120.

Leal, S.L., Yassa, M.A., 2015. Neurocognitive aging and the Hippocampus across species. Trends Neurosci. 38, 800–812.

Li, N., Sioutas, C., Cho, A., Schmitz, D., Misra, C., Sempf, J., Wang, M., Oberley, T., Froines, J., Nel, A., 2003. Ultrafine particulate pollutants induce oxidative stress and mitochondrial damage. Environ. Health Perspect. 111, 455–460.

Li, R., Navab, M., Pakbin, P., Ning, Z., Navab, K., Hough, G., Morgan, T.E., Finch, C.E., Araujo, J.A., Fogelman, A.M., Sioutas, C., Hsiai, T., 2013. Ambient ultrafine particles alter lipid metabolism and HDL anti-oxidant capacity in LDLR-null mice. J. Lipid Res. 54, 1608–1615.

Liu, Q., Babadjouni, R., Radwanski, R., Cheng, H., Patel, A., Hodis, D.M., He, S., Baumbacher, P., Russin, J.J., Morgan, T.E., Sioutas, C., Finch, C.E., Mack, W.J., 2016. Stroke damage is exacerbated by nano-size particulate matter in a mouse model. PLoS One 11, e0153376.

Magnusson, K.R., Cotman, C.W., 1993. Age-related changes in excitatory amino acid receptors in two mouse strains. Neurobiol. Aging 14, 197–206.

Matus-Amat, P., Higgins, E.A., Barrientos, R.M., Rudy, J.W., 2004. The role of the dorsal hippocampus in the acquisition and retrieval of context memory representations. J. Neurosci. 24, 2431–2439.

Misra, C., Kim, S., Shen, S., Sioutas, C., 2002. A high flow rate, very low pressure drop impactor for inertial separation of ultrafine from accumulation mode particles. J. Aerosol Sci. 33, 735–752.

Molinelli, A.R., Madden, M.C., McGee, J.K., Stonehuerner, J.G., Ghio, A.J., 2002. Effect of metal removal on the toxicity of airborne particulate matter from the Utah Valley. Inhal. Toxicol. 14, 1069–1086.

Morgan, T.E., Davis, D.A., Iwata, N., Tanner, J.A., Snyder, D., Ning, Z., Kam, W., Hsu, Y.T., Winkler, J.W., Chen, J.C., Petasis, N.A., Baudry, M., Sioutas, C., Finch, C.E., 2011. Glutamatergic neurons in rodent models respond to nanoscale particulate urban air pollutants in vivo and in vitro. Environ. Health Perspect. 119, 1003–1009.

Mumaw, C.L., Levesque, S., McGraw, C., Robertson, S., Lucas, S., Stafflinger, J.E., Campen, M.J., Hall, P., Norenberg, J.P., Anderson, T., Lund, A.K., McDonald, J.D., Ottens, A.K., Block, M.L., 2016. Microglial priming through the lung-brain axis: the role of air pollution-induced circulating factors. FASEB J 30, 1880–1891.

Ning, Z., Geller, M.D., Moore, K.F., Sheesley, R., Schauer, J.J., Sioutas, C., 2007. Daily variation in chemical characteristics of urban ultrafine aerosols and inference of their sources. Environ. Sci. Technol. 41, 6000–6006.

Ntziachristos, L., Ning, Z., Geller, M.D., Sioutas, C., 2007. Particle concentration and characteristics near a major freeway with heavy-duty diesel traffic. Environ. Sci. Technol. 41, 2223–2230.

Oberdörster, G., Sharp, Z., Atudorei, V., 2004. Translocation of inhaled ultrafine particles to the brain. Inhal. Toxicol. 16, 437–445.

Oller, A.R., 2002. Respiratory carcinogenicity assessment of soluble nickel compounds. Environ. Health Perspect. 110 (Suppl 5), 841–844.

Padurariu, M., Ciobica, A., Mavroudis, I., Fotiou, D., Baloyannis, S., 2012. Hippocampal neuronal loss in the CA1 and CA3 areas of Alzheimer's disease patients. Psychiatr. Danub 24, 152–158.

Power, M.C., Weisskopf, M.G., Alexeeff, S.E., Coull, B.A., Spiro 3rd, A., Schwartz, J., 2011. Traffic-related air pollution and cognitive function in a cohort of older men. Environ. Health Perspect. 119, 682–687.

Qin, L., Wu, X., Block, M.L., Liu, Y., Breese, G.R., Hong, J.S., Knapp, D.J., Crews, F.T., 2007. Systemic LPS causes chronic neuroinflammation and progressive neurodegeneration. Glia 55, 453–462.

Ranft, U., Schikowski, T., Sugiri, D., Krutmann, J., Krämer, U., 2009. Long-term exposure to traffic-related particulate matter impairs cognitive function in the elderly. Environ. Res. 109, 1004–1011.

Richwine, A.F., Parkin, A.O., Buchanan, J.B., Chen, J., Markham, J.A., Juraska, J.M., Johnson, R.W., 2008. Architectural changes to CA1 pyramidal neurons in adult and aged mice after peripheral immune stimulation. Psychoneuroendocrinology 33, 1369–1377.

Saffari, A., Daher, N., Shafer, M.M., Schauer, J.J., Sioutas, C., 2013. Seasonal and spatial variation of trace elements and metals in quasi-ultrafine (PM0.25) particles in the Los Angeles metropolitan area and characterization of their sources. Environ. Pollut. 181, 14–23.

Schauer, J.J., Lough, G.C., Shafer, M.M., Christensen, W.F., Arndt, M.F., DeMinter, J.T., Park, J.S., 2006. Characterization of metals emitted from motor vehicles. Res. Rep.-Health Eff. Inst. 1–76 discussion 77–88.

Serrano-Pozo, A., Frosch, M.P., Masliah, E., Hyman, B.T., 2011. Neuropathological alterations in Alzheimer disease. Cold Spring Harbor Perspect. Med. 1, a006189.

Tsien, J.Z., Huerta, P.T., Tonegawa, S., 1996. The essential role of hippocampal CA1 NMDA receptor-dependent synaptic plasticity in spatial memory. Cell 87, 1327–1338.

van Eeden, S.F., Tan, W.C., Suwa, T., Mukae, H., Terashima, T., Fujii, T., Qui, D., Vincent, R., Hogg, J.C., 2001. Cytokines involved in the systemic inflammatory response induced by exposure to particulate matter air pollutants (PM(10)). Am. J. Respir. Crit. Care Med. 164, 826–830.

Wellenius, G.A., Boyle, L.D., Coull, B.A., Milberg, W.P., Gryparis, A., Schwartz, J., Mittleman, M.A., Lipsitz, L.A., 2012. Residential proximity to nearest major roadway and cognitive function in community-dwelling seniors: results from the MOBILIZE Boston Study. J. Am. Geriatr. Soc. 60, 2075–2080.

Weuve, J., Puett, R.C., Schwartz, J., Yanosky, J.D., Laden, F., Grodstein, F., 2012. Exposure to particulate air pollution and cognitive decline in older women. Arch. Intern. Med. 172, 219–227.

WHO, 2009. Global Health Risks: Mortality and Burden of Diseases Attributable to Selected Major Risks. World Health Organization, Geneva. Available at: http://www.who.int/healthinfo/global_burden_disease/GlobalHealthRisks_report_full.pdf. Accessed August 2016.

Wise Sr., J.P., Wise, S.S., Little, J.E., 2002. The cytotoxicity and genotoxicity of particulate and soluble hexavalent chromium in human lung cells. Mutat. Res. 517, 221–229.

Zeng, Y., Gu, D., Purser, J., Hoenig, H., Christakis, N., 2010. Associations of environmental factors with elderly health and mortality in China. Am. J. Public Health 100, 298–305.

Zhang, H., Liu, H., Davies, K.J., Sioutas, C., Finch, C.E., Morgan, T.E., Forman, H.J., 2012. Nrf2-regulated phase II enzymes are induced by chronic ambient nanoparticle exposure in young mice with age-related impairments. Free Radic. Biol. Med. 52, 2038–2046.